SCS:en:lc F 37664.dec 1/21/93 PATENT

IN THE UNITED STATES PATENT AND TRADEMARK OFFICE

In re application of
John Dash and Patrick S. Keefe Art Unit
Serial No. 07/996,967
Filed: December 23, 1992
For: LOW TEMPERATURE NUCLEAR FUSION
Examiner:

DECLARATION PURSUANT TO 37 C.F.R. § 1.132

TO THE COMMISSIONER
OF PATENTS AND TRADEMARKS:

Sir:

1. I am a co-inventor on the application referenced above, which is a continuation application of U.S. patent application Serial No. 07/509,585, filed on April 16, 1990, entitled "Low Temperature Nuclear Fusion." I have read and understood the specification and claims of both of these applications.

2. I received a Bachelor of Science in Metallurgy from Pennsylvania State University in 1955. I then received a Masters degree in Metallurgy from Northwestern University in 1960. Finally, I received a Doctorate in Metallurgy from Pennsylvania State University in 1966.

3. I have had extensive training and experience in scientific research activities, including the physical and chemical aspects of electrochemistry, since at least as early as 1955. I have been a professor at Portland State University since 1966. I currently am employed as a full professor of physics at Portland State University. A copy of my resume is attached to this Declaration as Exhibit 1.

4. I have studied the work of Fleischmann and Pons and conducted research on the process they described since at least as early as 1989. I am quite familiar with the literature in this field.

Adequate Description in the Specification

5. Under my guidance, several devices have been assembled that are capable of producing heat energy as claimed in the parent and the continuation applications. These devices efficiently produce heat energy as discussed below.

The following steps were used in constructing these devices:

(a) An electrolyte container was selected. Page 2 of the specification, lines 12-15, states that a glass beaker can be used as long as it is inert to sulfuric acid and deuterated water;

(b) Stoppers then were inserted into the containers. See page 2 of the application, lines 15-17, and stoppers 14, 16 of the Drawing. These stoppers can be two-hole stoppers to provide a mounting for the electrodes. See the Drawing;

(c) An electrolyte was then formed using D_2O and H_2SO_4. A typical electrolyte had about 15% H_2SO_4 by volume. A particularly suitable electrolyte solution is described on page 4 of the application and consists of 20 ml. of heavy water (D_2O) with 3.5 ml. of sulfuric acid (specific gravity of 1.84). Page 4 of the application, lines 13-15;

(d) The electrolyte solution then was placed inside the container. The amount of the electrolyte solution used was

not critical, as long as a sufficient amount was used to at least partially cover the electrodes. This is shown in the Drawing;

(e) A cathode and anode then are placed inside the container. This is discussed on page 2 of the application, lines 18-20. Cathodes (22, 26) and anodes (20, 24) are shown in the Drawing.

A cold-rolled palladium cathode and a platinum anode were used. The specification particularly states that the cathode is "cold-rolled palladium" and that the anode is made from platinum. Page 2, lines 20-21. Furthermore, the specification states that the electrodes were cut from sheets of material. Page 4, lines 21-22.

The size of the anode and cathode are not critical. Nevertheless, a particularly suitable size of the cathode also is stated in the specification and is about 1 cm^2. Page 4, line 21. However, the actual size of the cathode can be larger as long as the relative size of the electrodes is maintained. The relative size of the electrodes also is stated. The platinum anode should have a surface area that is at least about 3 times that of the palladium cathode. Page 4, lines 19-22.

(f) A voltage then is provided across the cathode and anode. The applied voltage should be about 3.5 volts. Page 4, lines 23-25.

6. A device assembled as described above produces heat energy as claimed. The specification sufficiently describes all the critical parameters of the device including: (1) the container; (2) the composition and concentration of the electrolyte; (3) the composition of the electrodes; (4) the absolute size of a particular cathode and the relative sizes, in

terms of surface area, of the electrodes; and (5) the applied voltage. These parameters are sufficient to produce a device and use such device to practice a method that produces heat energy as claimed.

Production of Energy

7. Experiments were conducted by myself and co-inventor Patrick Keefe to demonstrate that a device assembled as described in Sections 5 and 6 above produces heat energy. These experiments have been meticulously repeated, taking care to eliminate experimental error.

8. Patrick Keefe used the device shown in Exhibits 2 and 3 (Figures 4 and 5 of his thesis) to evaluate the production of energy. The device shown in Exhibit 2 is identical to the device shown in the Drawing of the parent application as filed. Exhibit 3, which is a device used to evaluate the production of heat energy, has two of the devices shown in Exhibit 2 hooked in series to a source of electricity.

9. Using the device shown in Exhibit 3, Patrick Keefe obtained data regarding (a) the energy input versus experimental run time and (b) the temperature of the electrolyte versus experimental run time. The data obtained by Mr. Keefe from a first experiment is shown in attached Exhibit 4 (Figure 9 of Mr. Keefe's thesis). The data obtained from a second experiment is shown in attached Exhibit 5 (Figure 10 from Mr. Keefe's thesis).

Mr. Keefe did not stir the electrolyte when monitoring the temperature of the electrolyte. Electrolyte agitation occurred through the evolution of oxygen and hydrogen gases that are produced during electrolysis. This agitation was sufficient

to prevent any errors that may have been introduced by an electrolyte temperature gradient.

(a) Energy into the cell was calculated by multiplying cell voltage by current. The temperatures were determined by using a Copper-Constantan conversion table to convert thermocouple voltage into degrees Celsius. See attached Exhibit 6 (page 32 of Mr. Keefe's thesis).

(b) With reference to Exhibit 4, The Energy In vs. Run Time graph shows that the H-cell continually was run with a higher input energy (about 3%) relative to the D-cell. This higher energy input is achieved by adjusting the distance between the electrodes. However, because the H-cell and the D-cell are connected in series the input current for the two cells was the same.

(c) Again with reference to Exhibit 4, the higher energy input in the H-cell accounts for the higher temperature of the H-cell for the first 20 hours of the experiment as shown by the Temperature versus Run Time graph. However, after about 20 hours the temperature for the D-cell electrolyte equals the temperature of the H-cell electrolyte. More importantly, the Temperature versus Run Time graph of Exhibit 4 shows that during the last 15 hours of the experiment, the D-cell electrolyte maintained a higher temperature than the H electrolyte despite the fact that 3% less energy was put into the cell. The temperature of the D-cell was, on the average, 1°C above the H-cell and 1.8°C higher after 34 hours.

Thus, a D-cell, assembled as described in the specification of the parent application, produces heat energy in an efficient manner.

(d) To determine if these results were reproducible, Mr. Keefe repeated the experiment described above. The results of this experiment, which are shown in Exhibit 5, agree with the results shown in Exhibit 4. The energy input was consistently higher for the H-cell as shown by the Energy In versus Run Time graph of Exhibit 5. This explains the higher temperature for the H-cell for the first part of the experiment relative to the D-cell as shown by the Temperature versus Run Time graph of Exhibit 5. However, the temperature for the D-cell electrolyte surpasses the temperature for the H-cell after about 72 hours and thereafter is consistently higher than the temperature of the H-cell.

Mr. Keefe presented the data discussed herein to three respected scientists during his thesis defense. These scientists signed Mr. Keefe's thesis only after scrutinizing the data presented therein. The data presented by Mr. Keefe's thesis was sufficient to convince those of skill in the art as to the accuracy of the statements made therein. Mr. Keefe's results clearly demonstrate that the device described in the specification as originally filed, containing an electrolyte composition consisting of heavy water and sulfuric acid, consistently produces more energy than a cell containing water and sulfuric acid.

10. Elizabeth N. Nicholas, a graduate student working under my guidance, continued the research of Patrick Keefe to further verify the production of heat energy. The apparatus used by Ms. Nicholas is shown in Exhibit 7. This apparatus differs from Mr. Keefe's apparatus only in that it has a water jacket, designated as T, surrounding the electrolyte container. This

water jacket is not critical to the operation of the apparatus but rather is added to provide a stable temperature bath.

Attached Exhibits 8-14 describe the data obtained by Ms. Nicholas during the summer of 1990 in seven trials using the apparatus of Exhibit 7. All seven trials show that the D-cell produced significantly more heat energy than the H-cell. Thus, Ms. Nicholas' results provide additional support verifying the production of heat energy. Furthermore, Ms. Nicholas' results demonstrate that the highly efficient electrochemical reaction of the present invention can be repeatedly reproduced by practicing the apparatus and method described in the patent application as filed.

Ms. Nicholas also gathered data showing that the palladium cathode, which experiences significant surface morphology perturbations during electrolysis according to the present invention (see Section 12 below), has a lifetime of about 200 hours. After this period of time, the D-cell is no longer capable of producing more heat energy than the H-cell. This data is consistent with a heat-producing reaction that requires the palladium cathode electrolysis to produce the reaction-initiating reactants. Once the capability of the palladium cathode to produce these reactants is exhausted, the energy-producing reaction no longer proceeds.

D-cell Electrolyte Cools Slower than the H-cell Electrolyte

11. Exhibits 15 and 16 are cooling curves generated by Ms. Nicholas showing cooling profiles for the D-cell and the H-cell. The data for these cooling curves was compiled by measuring the temperature changes in the water jacket using a

thermocouple. Both Exhibits 15 and 16 show that the D-cell water bath initially had a higher thermocouple voltage, and hence initial temperature, than the H-cell. Thus, the initial D-cell temperature (arbitrarily designated T_{D1}) was greater than the initial H-cell temperature (T_{H1}) following removal of the voltage source.

a. The D-cell, which had substantially the same mass as the H-cell, should show a greater rate of temperature decrease from T_{D1} than the H-cell experienced from T_{H1} because T_{D1} is greater than T_{H1}. However, the Thermocouple Voltage versus Time After Power Off curves of Exhibits 15 and 16 show that the D-cell did not have a rate of temperature decrease that was greater than the H-cell.

b. The results stated above indicate that the heat-producing reaction of the D-cell continues to a greater extent than the reaction of the H-cell after the voltage source is disconnected from the electrodes. One possible explanation for this is based on the following: (1) the concentration of deuterium in the electrolyte appears to directly correlate with the extent to which the heat-producing reaction occurs; and (2) the production of the reactants required for the heat-producing reaction is initiated by electrolysis. These reactants remain in the palladium even after the voltage source is disconnected from the electrodes. Thus, the heat-producing reaction continues after the voltage source is disconnected, and does so to a greater extent in the D-cell than in the H-cell because the D-cell has a greater concentration of deuterium.

Exhibits 15 and 16 clearly show that the D-cell does not cool at a faster rate than the H-cell as would be expected if

a heat-producing reaction was not occurring in the D-cell. Hence, these results provide additional support for the conclusion that an energy-producing reaction is occurring to a greater extent in the D-cell than in the H-cell. Moreover, this result is reproducible as shown by the two Thermocouple Voltage versus Time After Power Off cooling curves of Exhibits 15 and 16.

Palladium Cathode Surface Analysis

12. Changes in the surface morphology of the palladium cathode following electrolysis according to the present invention show that a reaction occurs in the D-cell that is not occurring in the H-cell. The surface of palladium cathodes were examined following electrolysis in both H- and D-cells with the assistance of Mr. David S. Silver, Phillips Laboratory, Edwards Air Force Base. A document discussing the results of this investigation is attached hereto as Exhibit 17. This document has been submitted for publication.

(a) The document describes an electrolysis performed with a palladium cathode using an electrolyte containing both hydronium and deuterium ions. The cathode bends toward the anode during this process. After the electrolysis was complete, the cathode's concave surface was examined with a scanning electron microscope (SEM), an atomic force microscope (AFM), and a scanning tunneling microscope (STM). Examinations of D-cell cathodes showed evidence of localized surface melting on the cathode. See pages 8, 10 and 11 of Exhibit 17. Rimmed craters with faceted crystals inside were observed on the electrolyzed palladium cathode. These craters are not observed on palladium cathodes before they are electrolyzed in accordance

with the present invention, and such cratering does not usually occur in palladium cathodes during electrochemical reactions.

(b) The microscopic changes in the surface morphology of a palladium cathode appeared after electrolysis for 12 minutes in an electrolyte containing appreciable amounts of hydrogen ions along with deuterium ions. The surface craters observed with the SEM and AFM, especially, have characteristics such as stalagmites and rounded and faceted crystals which could be the result of localized melting. Height mode images and depth profiles showing rims around the craters suggest that molten material was ejected and solidified around the craters. Photos such as those shown in Exhibit 17, pages 8, 10, and 11, illustrate microscopic events which are reminiscent of large-scale events occurring after volcanic eruption.

(c) Other possibilities which could cause surface damage to the D-cell cathode include chemical interaction with the electrolyte or mechanical damage caused by the formation of palladium hydride or deuteride. Chemical interaction was ruled out by experiments which show that palladium is chemically inert in the electrolyte. Surface rupture might result from swelling caused by hydride or deuteride formation, but linear cracking, rather than cratering, would be the likely result.

(d) STM studies were performed ex situ of the surface of a palladium cathode after electrolysis in aqueous H_2SO_4 (1.5 mol dm^{-3}) for three hours with a constant cathodic current density of 500 mA cm^{-2}. The surface changed from smooth to nodular, but gave no evidence of cratering.

(e) When a control cell with electrolyte containing light water and sulfuric acid is electrolyzed in series with the

heavy water cell, the macroscopic distortion of the thin-foil palladium cathodes is of the same type in the two cells but much less in the light-water cell than in the heavy-water cell. Along with the greater distortion, the temperature of the heavy-water cell increases more than that of the light-water cell. These effects are quite reproducible. Thus, a heavy-water cell with a palladium cathode reproducibly undergoes more macroscopic distortion and generates more heat than an identical light-water cell connected in series with the same amount of power entering both cells. The distortion is apparently caused by compressive stresses on the cathode surface which faces the anode during electrolysis. Compressive stresses could be produced by porosity resulting from swelling of the lattice when hydrogen or deuterium is absorbed. Reaction of these gases with palladium results in formation of the beta phase, which has a lattice parameter about 3.6% larger than palladium. The cause of greater macroscopic distortion during heavy water electrolysis could be the observed cratering which may result from localized melting.

Dr. Schwinger's Hypothesis

13. Attached as Exhibit 18 is Dr. J. Schwinger's "Nuclear Energy in an Atomic lattice. I," Z. Phys. D., 15:221-225 (1990). In 1965, Dr. Schwinger won the Nobel prize for theoretical physics. Dr. Schwinger's article states that the release of energy by electrolyzing heavy water could be true, but that the likely product would be ^{3}He plus heat energy, and not ^{4}He and heat energy. Dr. Schwinger postulates that the dominant process that occurs during the electrolysis is an HD interaction, leading to the formation of ^{3}He, and not a DD

interaction that leads to the formation of ^4He.

Dr. Schwinger's paper provides a possible explanation as to why the present application provides unexpectedly superior results when compared to other similar processes. Dr. Schwinger postulates that the energy-producing reaction of the D-cell is facilitated by the presence of hydronium ions. In the present application, the sulfuric acid supplies the hydronium ions.

Eliminating Experimental Error

14. Care was taken during the experiments described herein and in the patent applications to minimize experimental errors. These precautions include:

(a) allowing the electrolyte solution to equilibrate, thereby at least partially accounting for any errors that may be introduced by temperature gradients;

(b) monitoring the temperature of the cells in various locations to insure that no "hot spots" were occurring. The readings for Ms. Nicholas' data were taken with the tip of the water-jacket thermocouple placed in each beaker about 2.3 cm above the bottom surface of the beaker. However, to investigate the occurrence of hot spots, the thermocouple was systematically moved to various locations in the cooling bath to obtain temperature readings at the various locations. This data is shown in Exhibit 19. The thermocouple readings can be converted into temperature readings using a conversion factor of 25°/1 mV. The data of Exhibit 19 shows that the temperature difference between readings was never greater than about 1.25° (0.05 mV) and was typically less than about 0.5° (0.02 mV). Thus, the greatest possible difference between temperature readings that could

result from a temperature gradient cannot account for the difference in heat energy produced by the H-cells and the D-cells, especially when considering that the D-cells continuously had at least about 3% and up to about 6% less input energy that did the H-cells;

(c) monitoring the temperature of the cells using sensitive chart recorders; and

(d) switching the leads to the temperature recording units to verify that the readings were consistent.

The Utility of Producing Heat Energy by the Method of the Present Invention

15. A D-cell made according to the present invention produces a significant amount of energy. For instance, if a 25×10^{-4} cm^3 palladium cathode is used, the D-cell produces about 0.25 watts of excess energy relative to the H-cell. Hence, this system produces about 100 watts/cm^3 (0.25 watts divided by 25×10^{-4} cm^3), and does so for a period of about 200 hours. In comparison, a normal flashlight battery provides only about 10 watts for a period of about 10 hours. Hence, the energy production of an invention according to the present application is superior to many of the energy-producing batteries currently in use.

I hereby declare that all statements made herein of my own knowledge are true and that all statements made on information and belief are believed to be true; and further that these statements were made with the knowledge that willful false statements and the like so made are punishable by fine or imprisonment, or both, under Section 1001 of Tile 18 of the United States Code and that such willful false statements may

jeopardize the validity of the application or patent issued thereon.

1-21-93
Date

John Dash

CURRICULUM VITA

John Dash

EDUCATION

B.S. Pennsylvania State University, 1955
M.S. Northwestern University, 1960
Ph.D Pennsylvania State University, 1966

PROFESSIONAL EXPERIENCE

1955-1958	Research Metallurgist, Crucible Steel Company, Midland, PA
1960-1963	Research Associate, Res, Inst. for Advanced Study, Baltimore, MD
1963-1965	Teaching Assistant, Pennsylvania State University
1966-1971	Assistant Professor, Portland State University
1971-present	Professor, Portland State University
1985-present	President, Electrochemical Innovations, Inc.

RESEARCH AND TEACHING FIELDS

Research Fields:
Electrolytic Reaction, Phase Transformations, Electron Microscopy

Teaching:
Electron Microscopy, Physical Metallurgy, Thermodynamics, Environmental Sciences and Resources

PUBLICATIONS RELATED TO ELECTROLYTIC REACTIONS

1. "Magnetic stirring during electrolytic thinning," Proceedings of the Electron Microscopy Society of America, St. Paul, 1969 (Baton Rouge, Claitor's Book Store, 1969), p. 144.

2. "Electrodeposition of metals in magnetic fields," Proceeding of the Electron Microscopy Society of America (Baton Rouge, Claitor's Book Store, 1971), with W.W. King.

3. "Electrothinning and electrodeposition of metals in magnetic fields," J. Electrochem. Soc. 119, 51 (1972), with W.W. King.

4. "Influences of magnetic fields on the energy output of Leclanche cells," Extended Abstracts of the Electrochemical Society 71-2, p. 45, Dallas, TX, October 1975, with W. Socha.

5. "Effects of magnetic fields on the structure of electrodeposited copper," Proc. 38th Annual Meeting of EMSA, San Francisco, 1980 (Baton Rouge, Claitor's Publishing Div.) p. 144, with K. Housen.

6. "Use of AS1 for increasing the current efficiency of chromium plating," Invention Report, PSU 1980, with A. Kasaaian.

7. "Improving efficiency of Cr plating with higher sulfate and Cr (III)," AES 69th Annual Technical Conference Proceedings, Vol. 2, Paper U4, San Francisco, June 1982, with A. Kasaaian.

8. "Use of alcohol for increasing the current efficiency of chromium plating," U.S. Patent No. 4,447,299 with A. Kasaaian. Application also filed for Canadian patent.

9. "Influence of magnetic fields on the electrodeposition of chromium," AES 70th Annual Technical Conference Proceedings, Vol. 1, Paper A4, Indianapolis, June 1983, with Ru-Tsin Chen and K. Housen.

10. "Effect of magnetic fields on the morpohology of electrodeposited copper," Proc. 41st Annual Meeting of EMSA, Phoenix, 1983 (San Francisco Press), with H. Takeo and S. Mal.

11. "Effect of magnetic fields and flow applied to single electrodes on electrolytic cell potentials," J. Appl. Phys. 55, 2604 (1984), with M. Takeo.

12. "The effect of magnetic fields applied during aqueous electrolysis on circulation and on electrode processes," J. Appl. Phys. 55, 2060 (1984), with C. Cousins and C. Gorg.

13. "Magnetic effects on electroplating of copper," Proc. AES 11th Plating in the Electronics Industry Symposium, Orlando, Feb. 1984, with H. Takeo and C. Tam.

14. "High efficiency chromium and chromium-iron plating," AES 71st Annual Technical Conf. Proc., NY, July 1984, with A. Kasaaian.

15. "SEM and EDS study of magnetic effects on electroplating of Cr-Fe alloys," Proc. 42nd Annual Meeting of Electron Microscopy Society of America, (San Francisco Press, 1984) p. 502 with C. Cousins.

16. FILM: "Effects of magnetic fields on aqueous electrolysis," with C. Cousins and C. Gorg, 1983.

17. "Use of alcohol for increasing the current efficiency and quality of chromium-iron alloy plating," Patent Application filed in Great Britain and France, with A. Kasaaian.

18. "Chromium-iron alloy plating using hexavalent and trivalent chromium ion solutions," U.S. Patent 4,615,773, with A. Kasaaian.

19. "Effect of methanol and formic acid on chromium plating," Plating and Surface Finishing 71, No. 11, 66 (Nov. 1984), with A. Kasaaian.

20. "Effects of chromium electroplating solution composition on properties of the deposits," AES 72nd Annual Technical Conference Proceedings, paper P4, Detroit, July 1985, with A. Kasaaian and W.F. Lanford.

21. "Electrolytic codeposition of alumina with copper in a magnetic field," Extended Abstracts, Electrochemical So., Las Vegas, Oct. 1985, with J. Anderton, B. Litzenberger and A. Trzynka.

22. "Codeposition of metals and nonmetallic particles," U.S. Patent, May 1987.

23. "Chromium plating from a solution containing Cr (VI), Cr (III), and Iron," Proc. Int. Chromium Colloquium, San Diego, CA, Feb. 1987, with A. Kasaaian and M. Hotchkiss.

PROFESSIONAL SOCIETIES

American Society for Metals - member since 1955; Chairman, Penn State Chapter, 1965-66; Chairman, Oregon Chapter, 1977-78.

American Electroplaters' Society - member since 1980; Chairman, Education Committee 1983-86.

Electron Microscopy Society of America - member since 1962.

Sigma Xi - member since 1965.

AWARDS

American Electroplaters' Society Silver Medal Award for outstanding paper published in Plating and Surface Finishing during 1984, with A. Kasaaian.

Oregon Museum of Science and Industry Award for research on Electrolysis in Magnetic Fields (1971).

Analyzed (Sp.G. 1.84), was allowed to equilibrate for 24 hours.

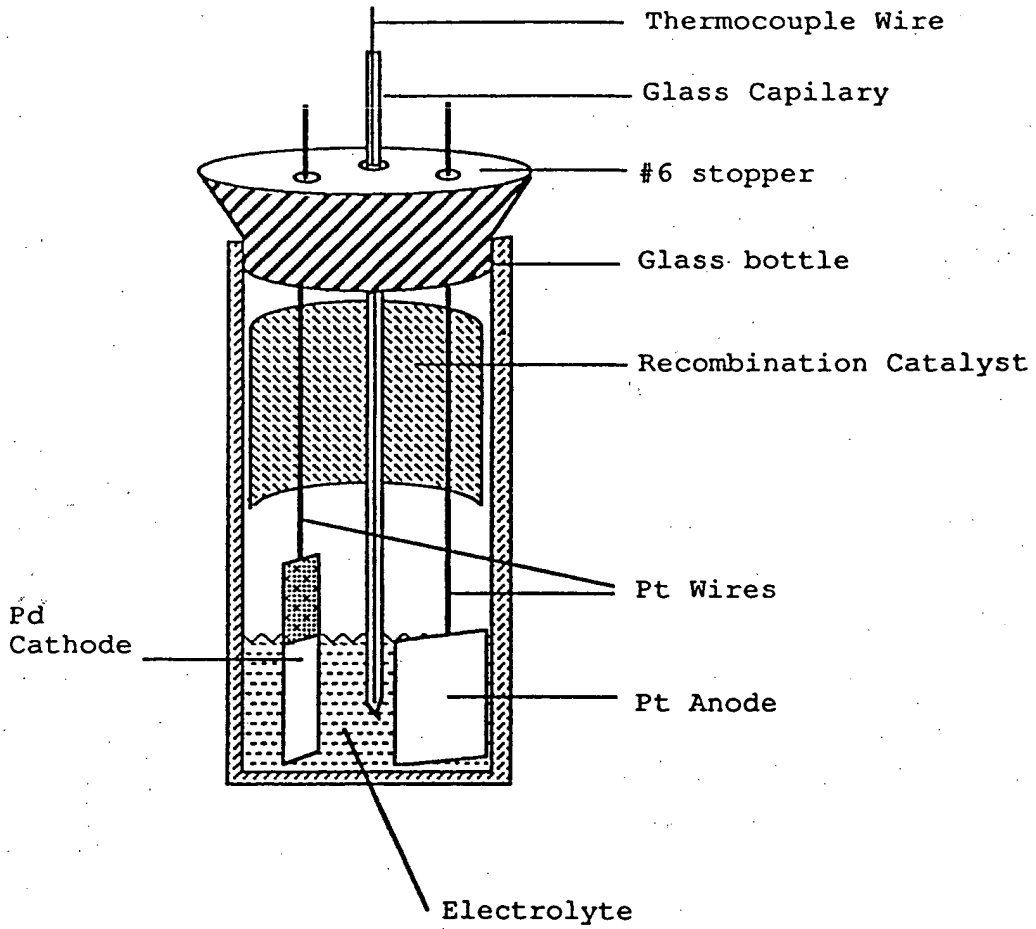

Figure 4. Electrolysis cell design used in Experiment One.

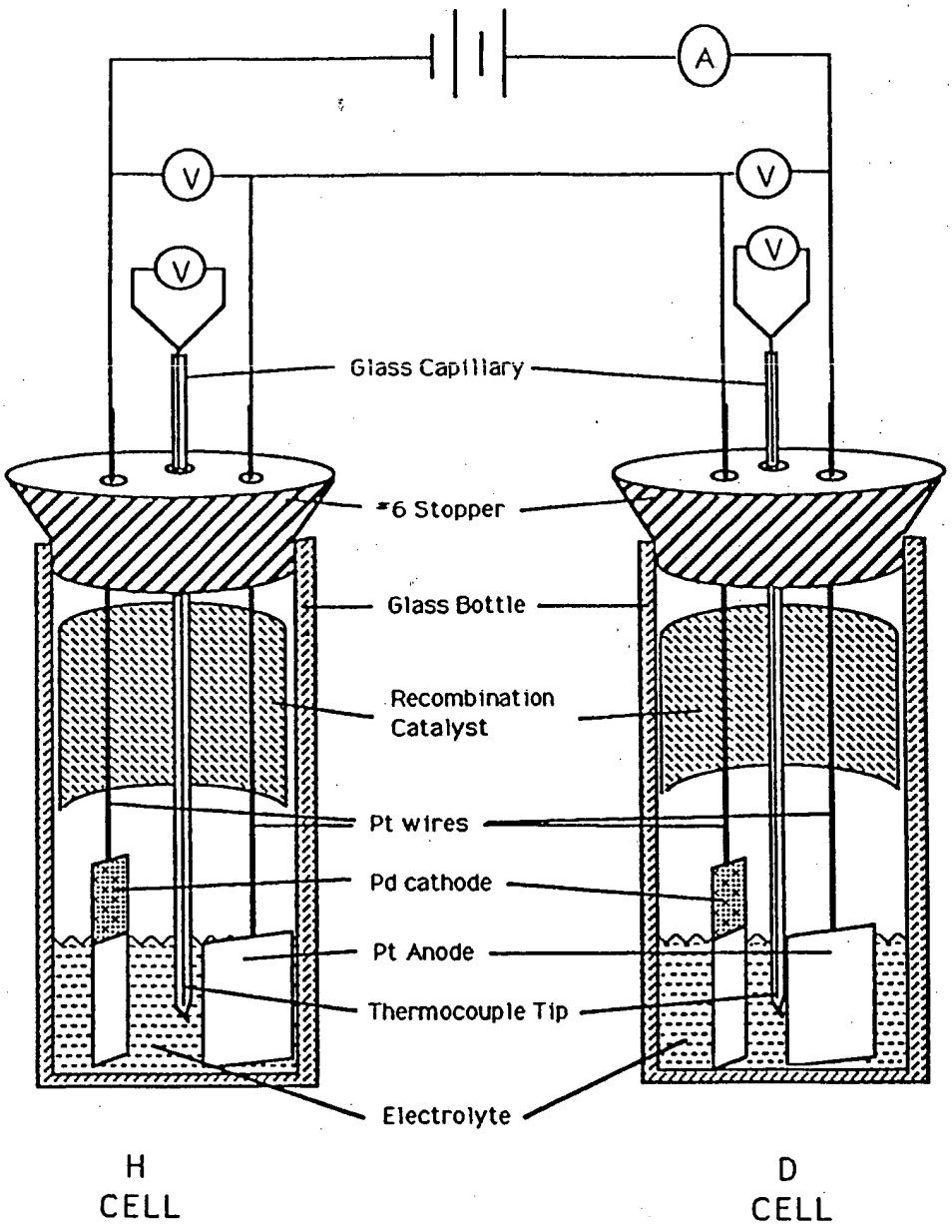

Figure 5. Diagram of experimental set-up for Experiment One.

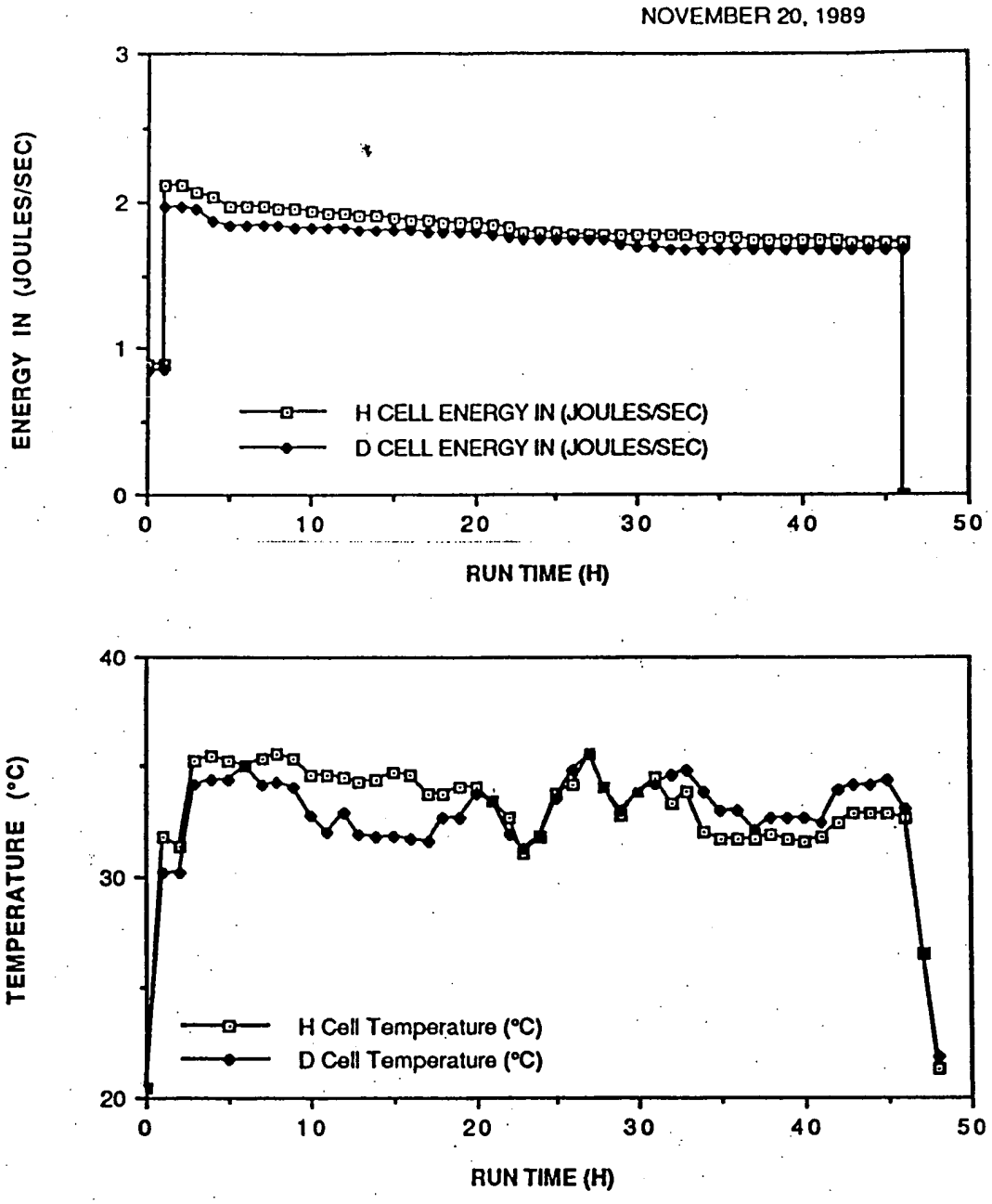

Figure 9. Energy In vs Run Time and Temperature vs Run Time for Experiment One.

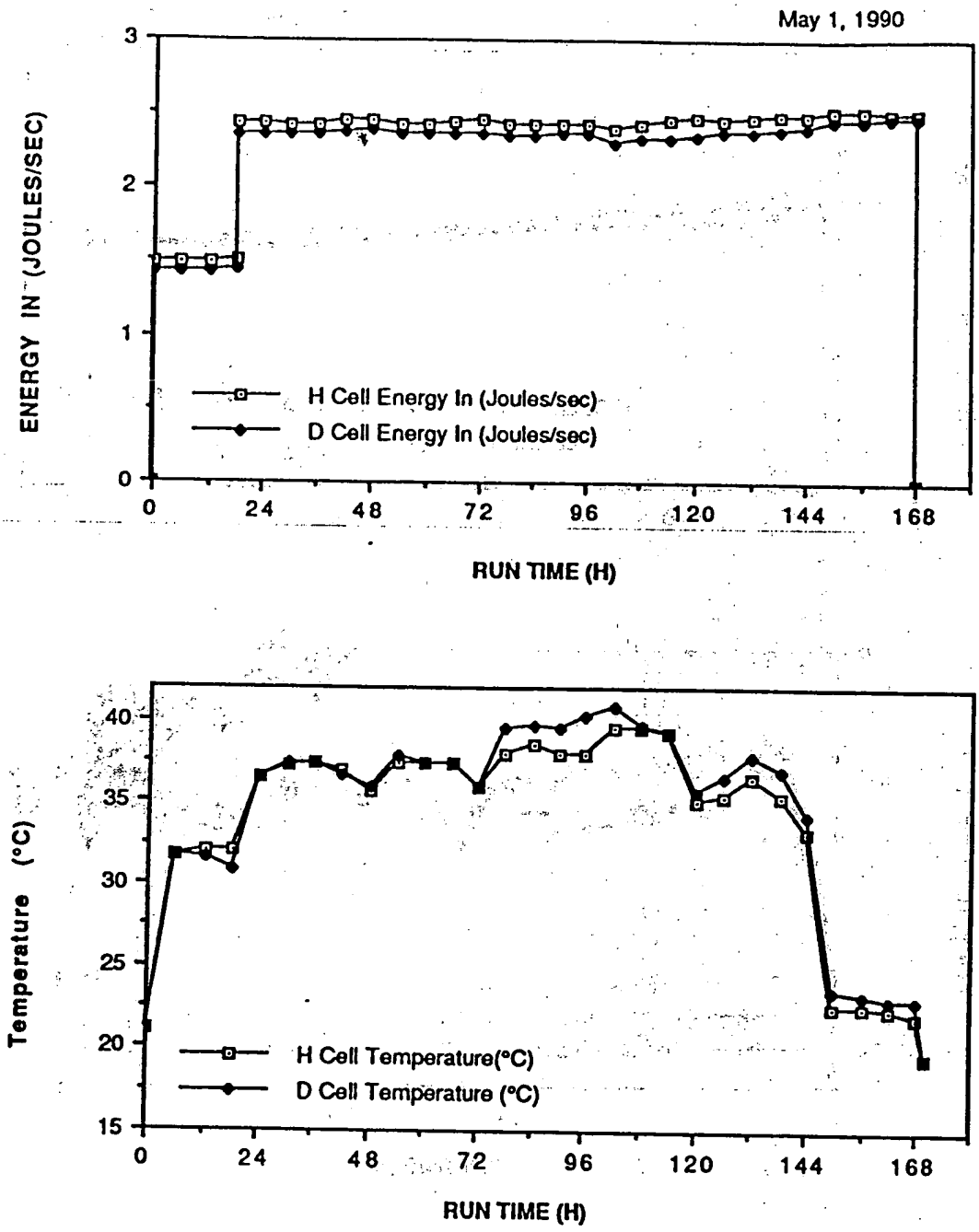

Figure 10. Energy In vs Run Time and Temperature vs Run Time for Experiment Two.

Energy In was calculated by multiplying cell voltage by current. Temperatures were determined by using a Copper-Constantan conversion table to convert thermocouple voltage into degrees Celsius and then adjusting for room temperature.

The Energy In vs. Run Time graph shows that the H cell was continually run with a higher input energy, approximately 3%. Since the cells were in series, the current was the same for the two cells, but the voltage across the H cell was higher then the voltage across the D cell. This higher input of energy accounts for the fact that the H cell maintained a higher electrolyte temperature for the first 20 hours of the experiment. The current was a constant 0.5 A for the first 2 hours and then 0.75 A for the remainder of the experiment.

The Temperature vs Run Time graph shows that from 20 to 30 hours, the H and D electrolyte temperatures jumped around with the changes in the room temperature, but remained approximately equal. During the last 15 hours of the experiment, the D cell electrolyte maintained a higher temperature then the H electrolyte despite the fact that 3% less energy was being put into the cell. The temperature of the D cell was on the average 1°C above the H cell and 1.8°C higher after 34 hours of electrolysis.

The cells were allowed to cool down after the electrical power was turned off. The two cells cooled down at the same rate at the same temperatures.

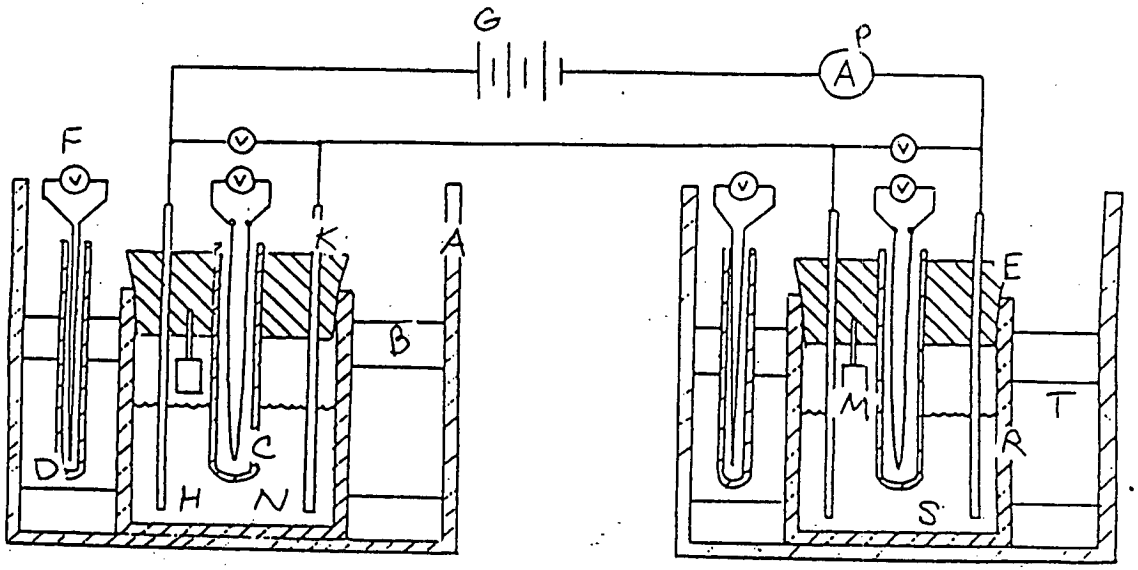

A -- glass beaker
B -- styrofoam ring
C -- thermocouple
D -- glass capillary tube
E -- rubber stopper
F -- voltage meter
G -- power source
H -- Pd cathode

K -- Pt anode
M -- recombination catalyst
N -- electrolyte (H20)
P -- ammeter
R -- glass bottle
S -- electrolyte (D20)
T -- water jacket

Figure 1. Experimental setup.

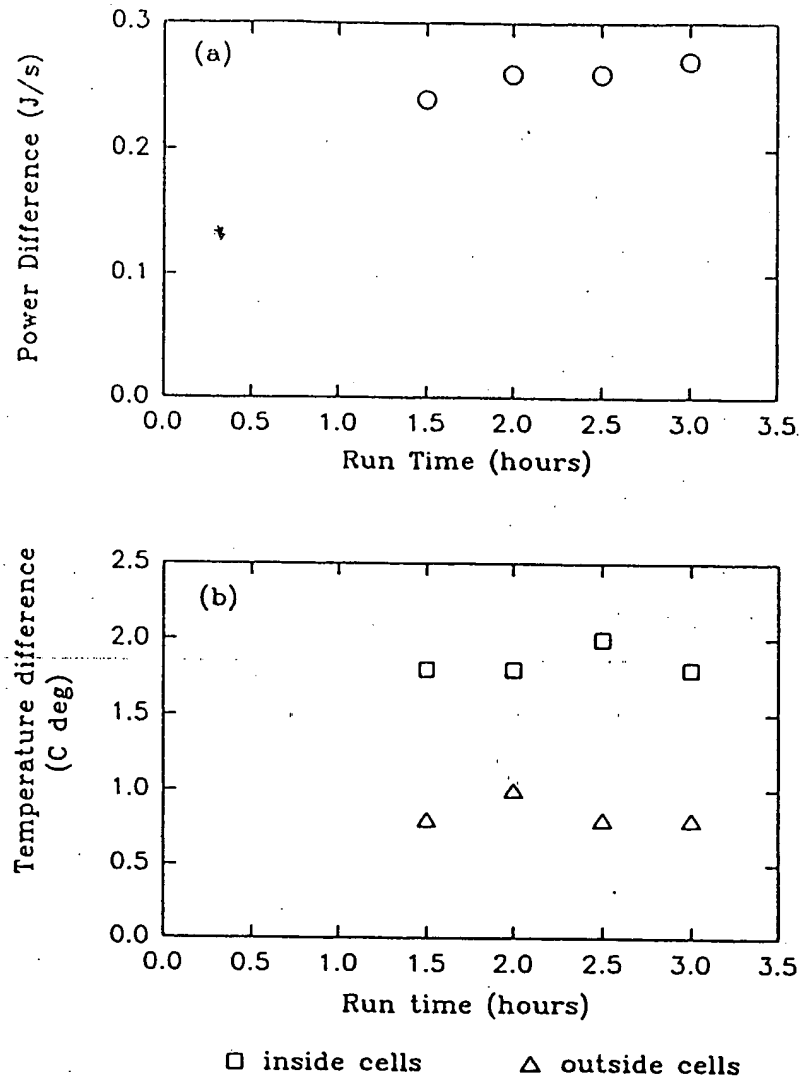

Figure 2. (a) Power supplied to H_2O cell minus power supplied to D_2O cell, versus time. Difference between cell voltages was about 0.2 V, and current was about 1.3 A. (8-13-90) (b) Temperature of D_2O cell minus temperature of H_2O cell, versus time. (8-13-90)

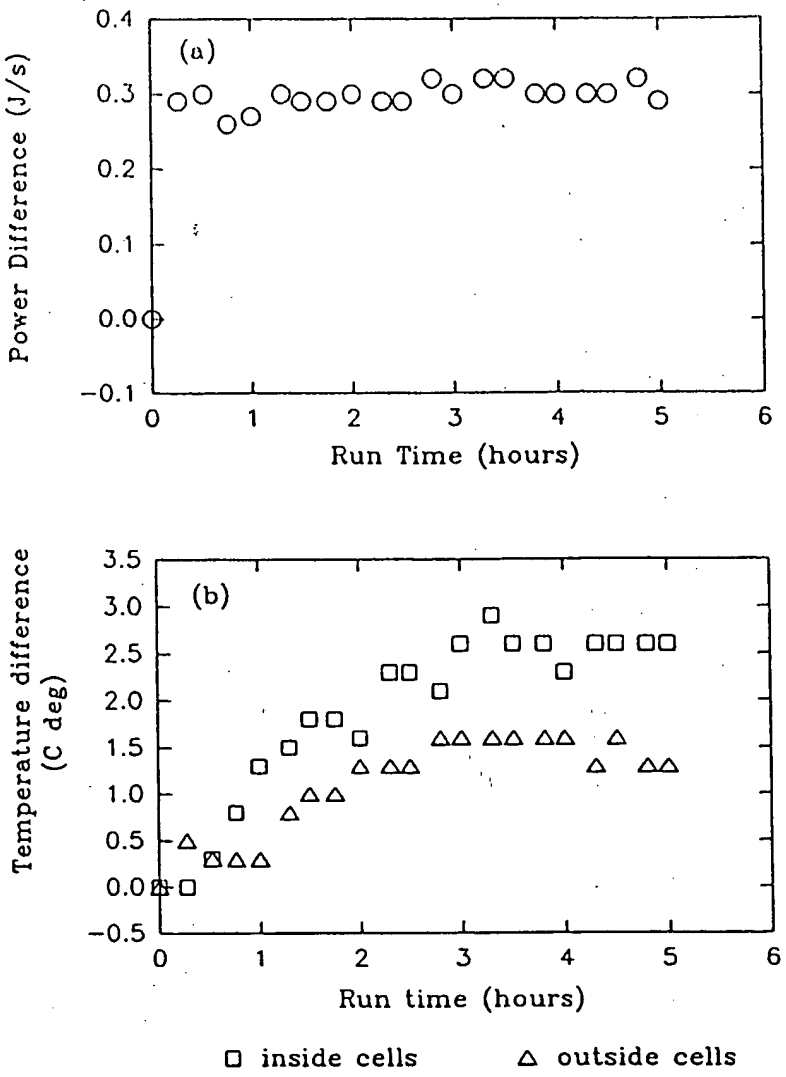

Figure 3. (a) Power supplied to H_2O cell, minus power supplied to D_2O cell, versus time. Difference between cell voltage was about 0.2 V, and current was 1.5 A. (8-14-90) (b) Temperature of D_2O cell minus temperature of H_2O cell, versus time. (8-14-90)

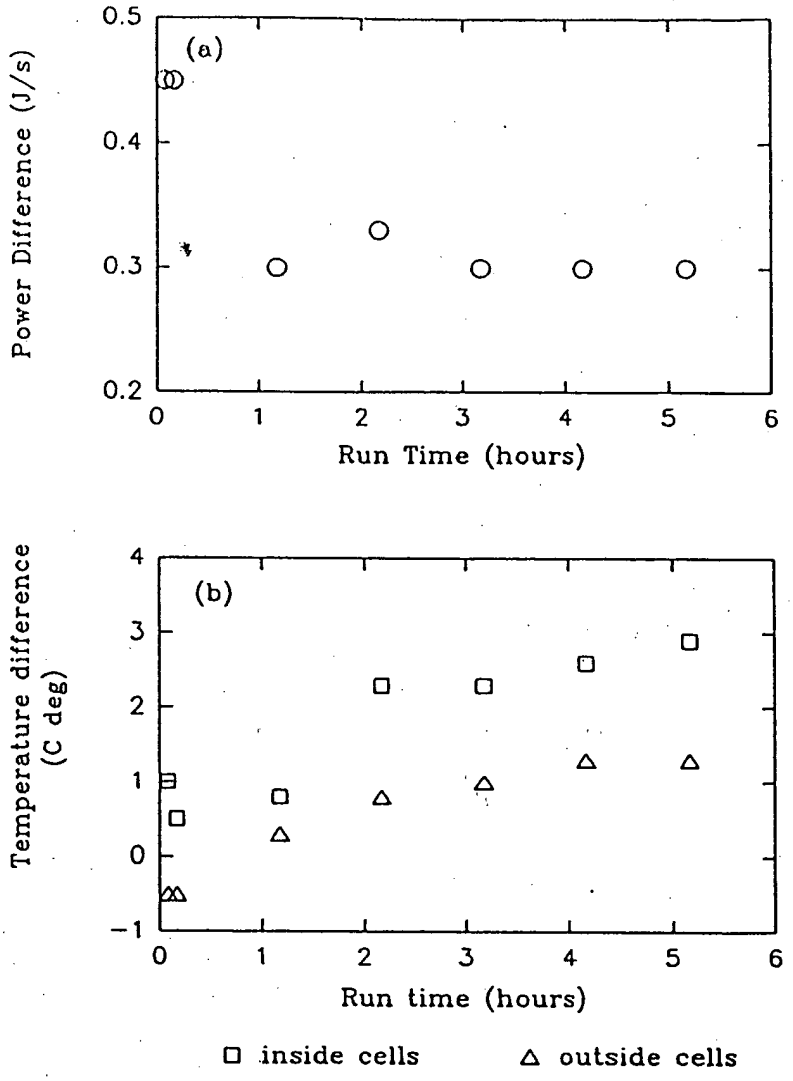

Figure 4. (a) Power supplied to H_2O cell minus power supplied to D_2O cell, versus time. Difference between cell voltages was about 0.2 V, and current was 1.5 A. (8-16-90) (b) Temperature of D_2O cell minus temperature of H_2O cell, versus time. (8-16-90)

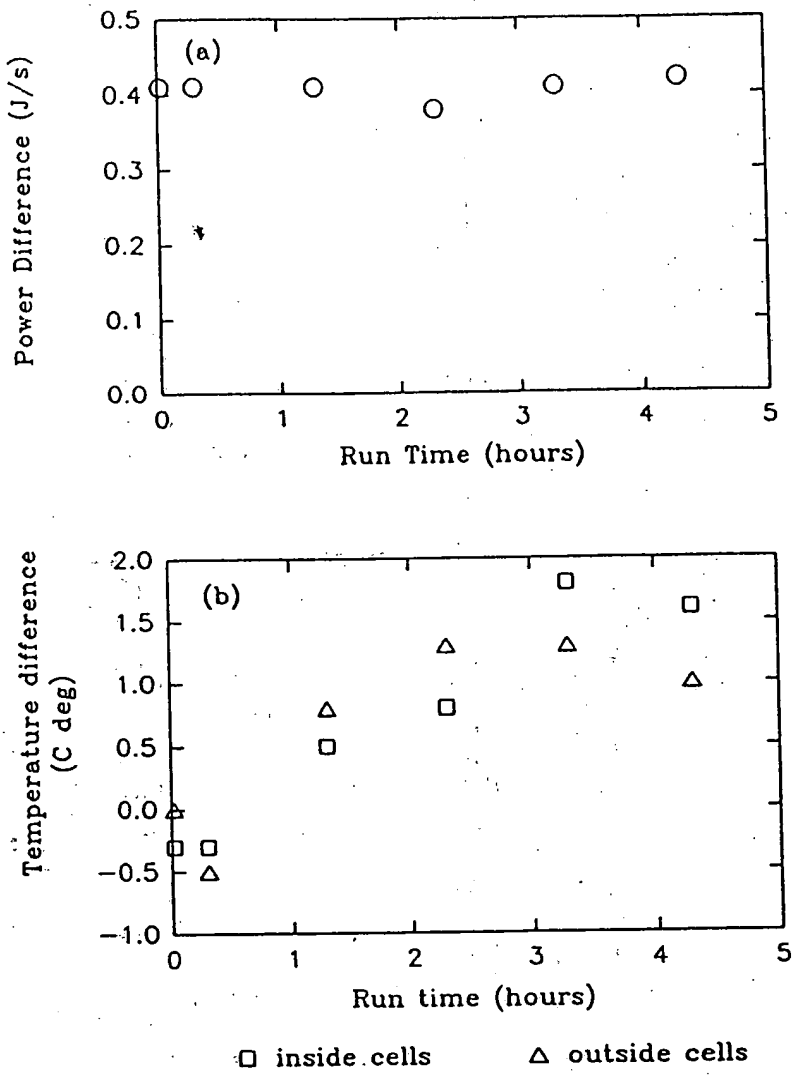

Figure 5. (a) Power supplied to H_2O cell minus power supplied to D_2O cell, versus time. Difference between cell voltages was about 0.25 V, and current was about 1.5 A. (8-20-90) (b) Temperature of D_2O cell minus temperature of H_2O cell, versus time. (8-20-90)

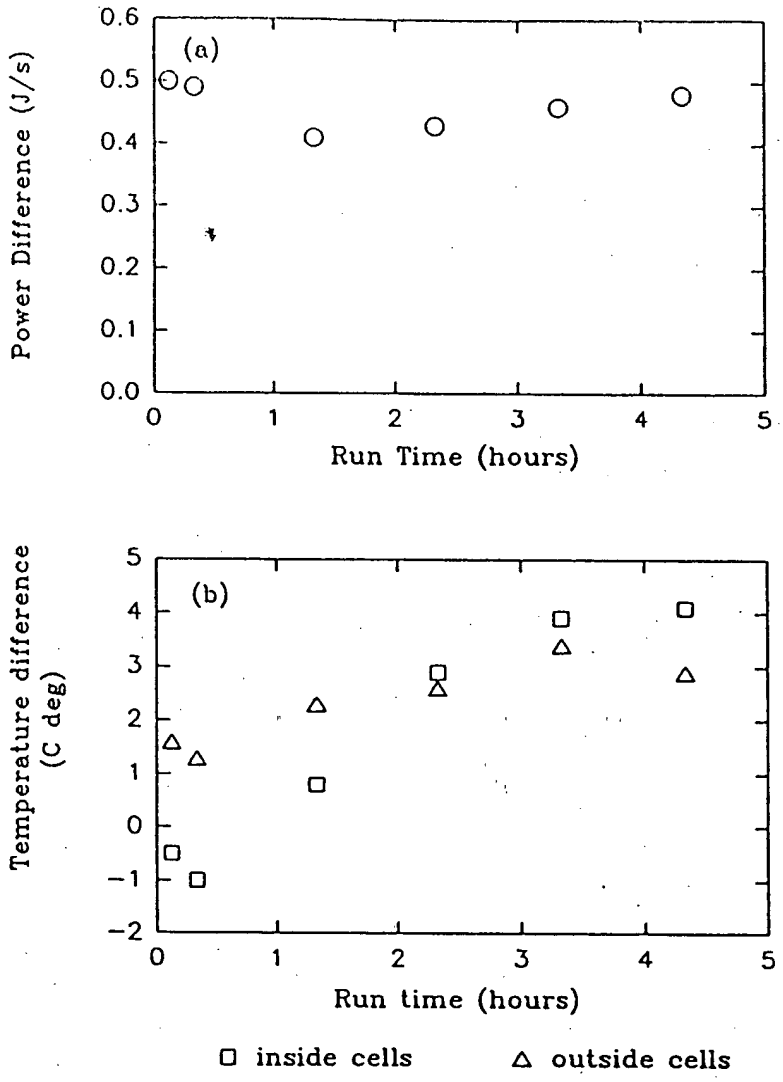

Figure 6. (a) Power supplied to H_2O cell, minus power supplied to D_2O cell, versus time. Difference between cell voltages was about 0.25 V, and current was 1.7 A. (8-21-90) (b) Temperature of D_2O cell minus temperature of H_2O cell, versus time. (8-21-90)

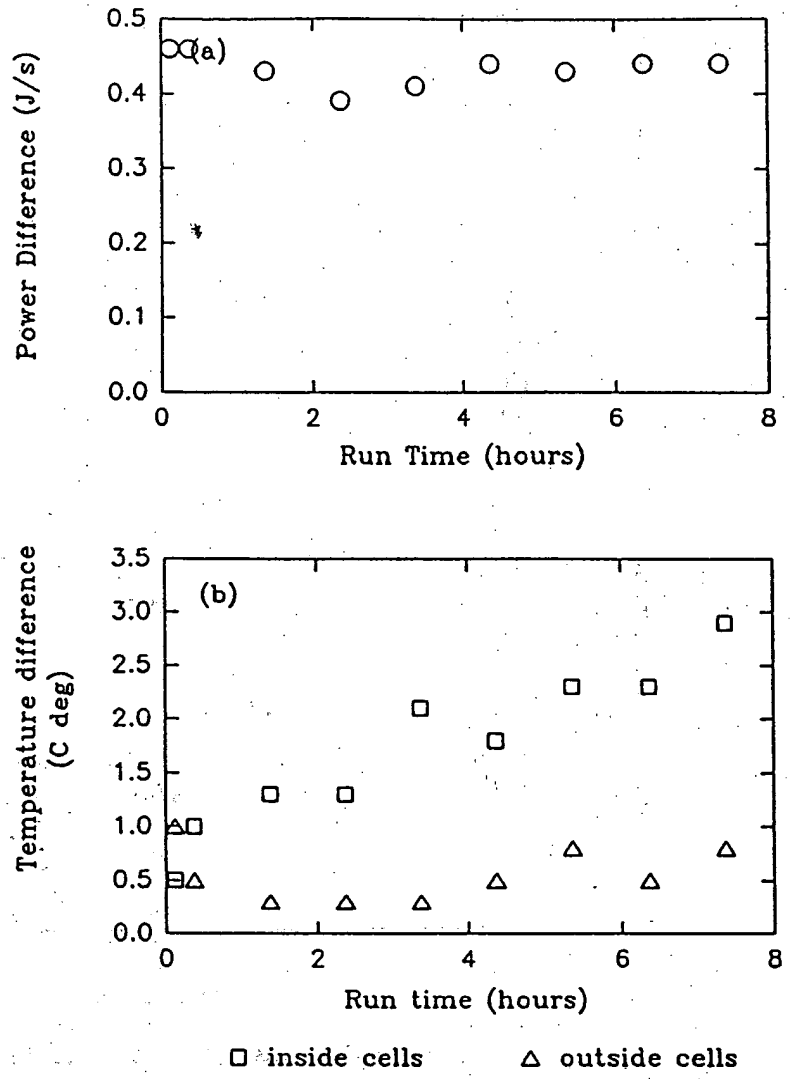

Figure 7. (a) Power supplied to H_2O cell, minus power supplied to D_2O cell, versus time. Difference between cell voltages was about 0.2 V, and current was 1.7 A. (8-23-90) (b) Temperature of D_2O cell minus temperature of H_2O cell, versus time. (8-23-90)

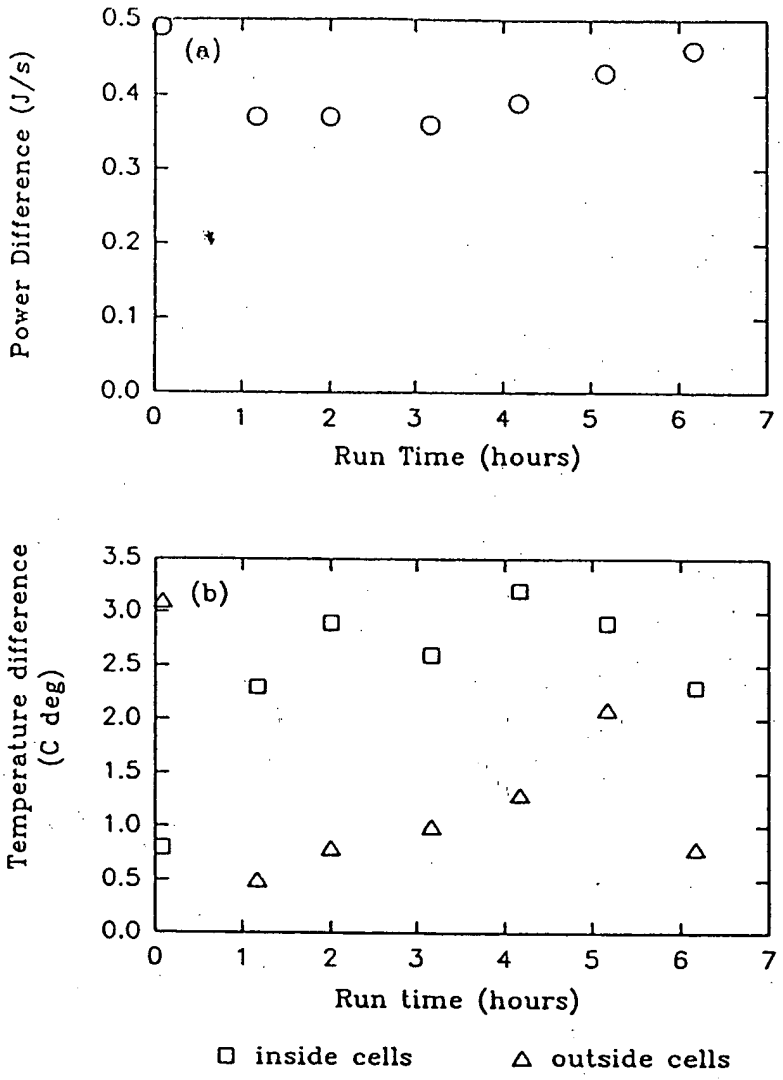

Figure 8. (a) Power supplied to H_2O cell, minus power supplied to D_2O cell, versus time. Difference between cell voltages was about 0.2 V, and current was 1.7 A. (8-27-90) (b) Temperature of D_2O cell minus temperature of H_2O cell, versus time. (8-27-90)

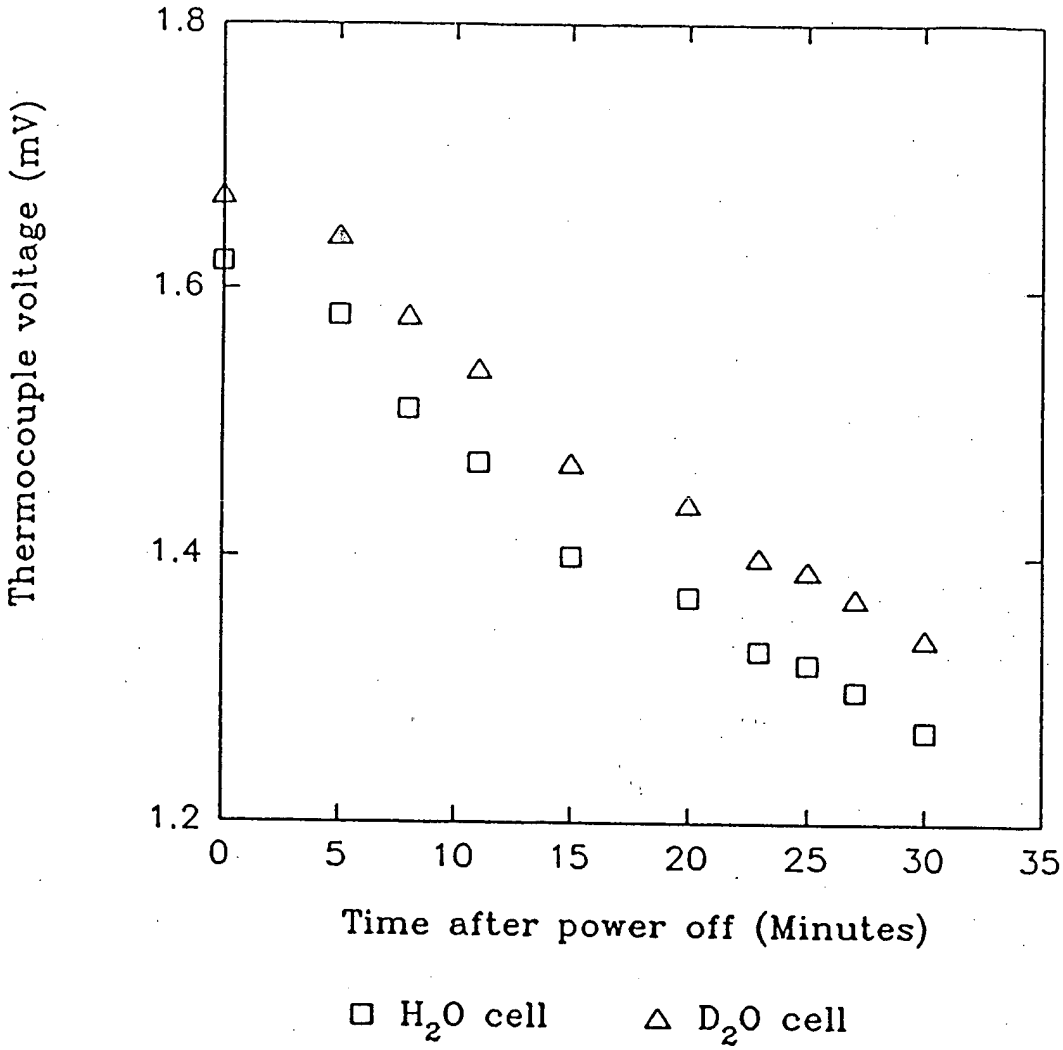

Figure 9. Thermocouple voltages in the outer water jackets. Cooling curve. (8-14-90)

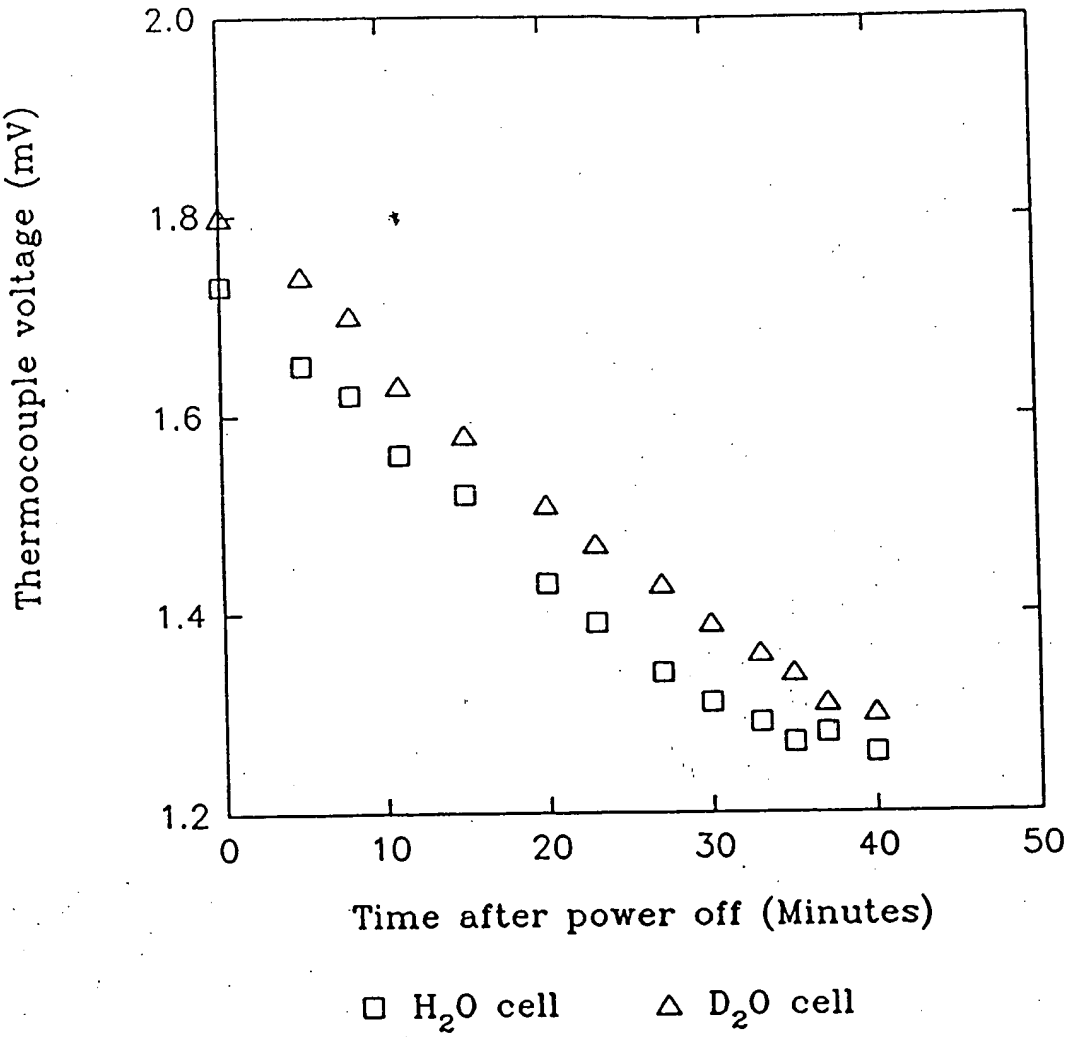

Figure 10. Thermocouple voltages in the outer water jackets, Cooling curve. (8-27-90)

Submitted for publication.

EVIDENCE FOR LOCALIZED SURFACE MELTING ON A Pd CATHODE ELECTROLYZED IN HEAVY WATER

David S. Silver
Phillips Laboratory
Edwards AFB, California

and

John Dash and Patrick S. Keefe
Physics Department, Portland State University
P.O. Box 751, Portland, OR 97207

ABSTRACT

Electrolysis was performed with a palladium cathode and an electrolyte containing both hydrogen and deuterium ions. The cathode bends toward the anode during this process. Examination of the concave surface with SEM, AFM, and STM shows evidence for localized surface melting. Rimmed craters with faceted crystals inside were observed on an electrolyzed palladium cathode but not on palladium which had not been electrolyzed.

INTRODUCTION

The phenomena which occur during the electrolysis of heavy water with a palladium cathode have been studied extensively since the reports of the possibility of nuclear fusion in this process (1, 2). It has been suggested that nuclear fusion may occur in this system by the combination of H and D rather than D and D, and that the energy released may be absorbed by the palladium lattice (3).

In the work reported here, a large amount of H is produced at the cathode along with D. Microscopic features produced on the palladium surface have been characterized using the SEM, AFM, and STM.

EXPERIMENTAL METHODS AND RESULTS

The electrolyte used in this experiment contained 20 ml D_2O and 3.5 ml H_2SO_4 (Sp. G 1.84). Pd foil about 25 μm thick was produced by cold rolling Pd from a rod to about 90% reduction in thickness. The Pd foil was scratched on the surface, and the area of the scratch was photographed, Fig. 1a. The foil was then immersed in the electrolyte for one hour. The same area was then photographed, Fig. 1b. Because there was no observable change on the surface and no weight change, it was concluded that the Pd foil was chemically inert in the electrolyte.

a

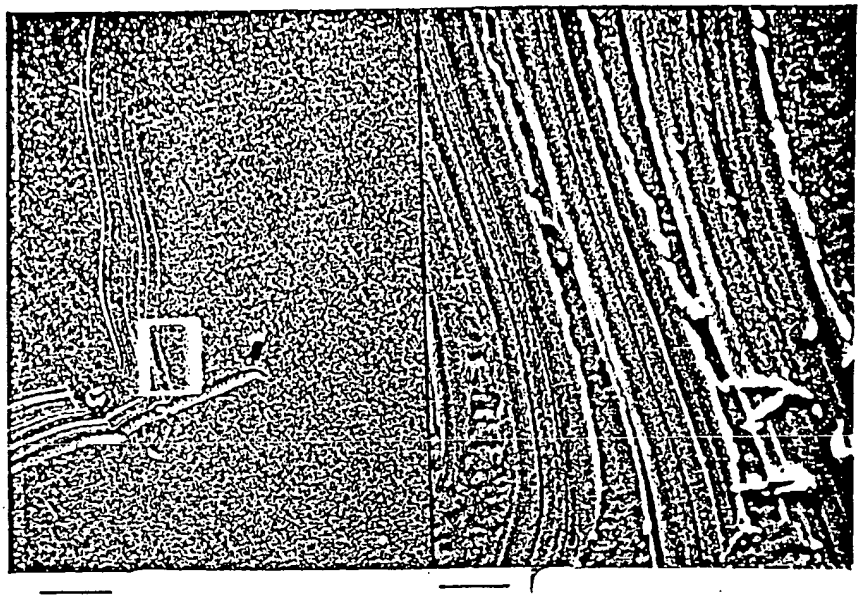

b

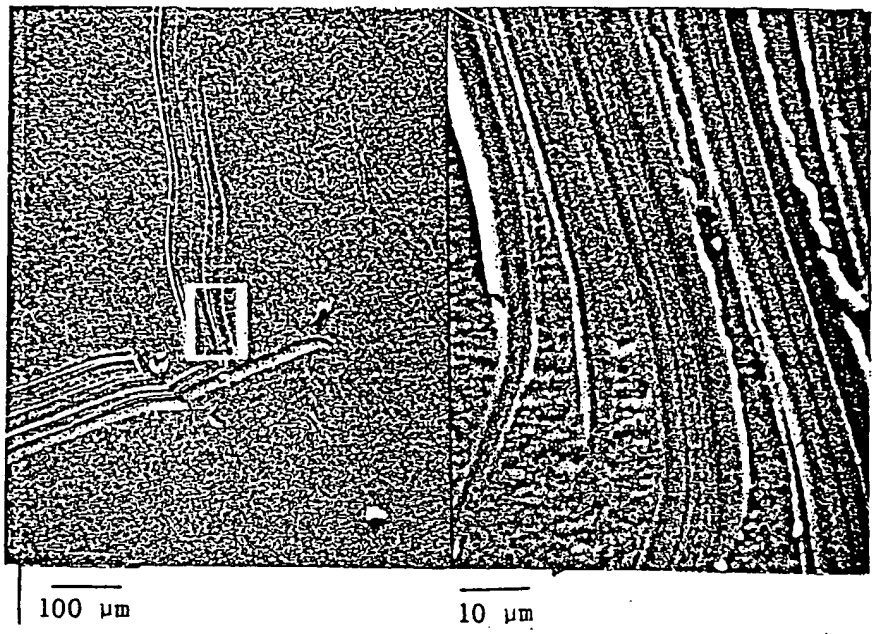

Fig. 1 SEM micrographs of the same area of the Pd cathode before (a) and after (b) immersing in the electrolyte for one hour in order to determine if the chemicals in the electrolyte had any reaction with Pd. There was no weight change and it appears that there was no chemical reaction.

The Pd cathode used for electrolysis was made by cold rolling a high purity single crystal from about 250 μm to 25 μm thickness. Pt foil was used for the anode. Electrolysis was performed at room temperature, using a 50 ml beaker to contain the electrodes and electrolyte. Constant current of 0.5 A and a cathode current density of about 0.25 A/cm^2 was passed for 12 minutes. The cell voltage was about 3.5 V. The Pd cathode rapidly distorted during electrolysis, causing it to become bent toward the Pt anode. After electrolysis, this was examined with a scanning electron microscope on the side which faced the anode. Surface damage such as that shown in Fig. 2 was observed.

In addition to the large pit with stalagmites inside, there are smaller pits randomly scattered over the surface. The electrolyte temperature rose during electrolysis, but there was no control cell in series for comparative temperature measurements. An EDS spectrum of the surface showed that only Pd was present.

Small surface pits, such as that indicated by the arrow on Fig. 2, were examined with the scanning tunneling microscope (STM) and with the atomic force microscope (AFM). As a control, a piece of the cold rolled single crystal foil not used in electrolysis was also examined in the STM and AFM.

The AFM observations were accomplished in air at normal room temperatures using a Nanoscope II microscope. Observations were generally made using two different image modes, one being the

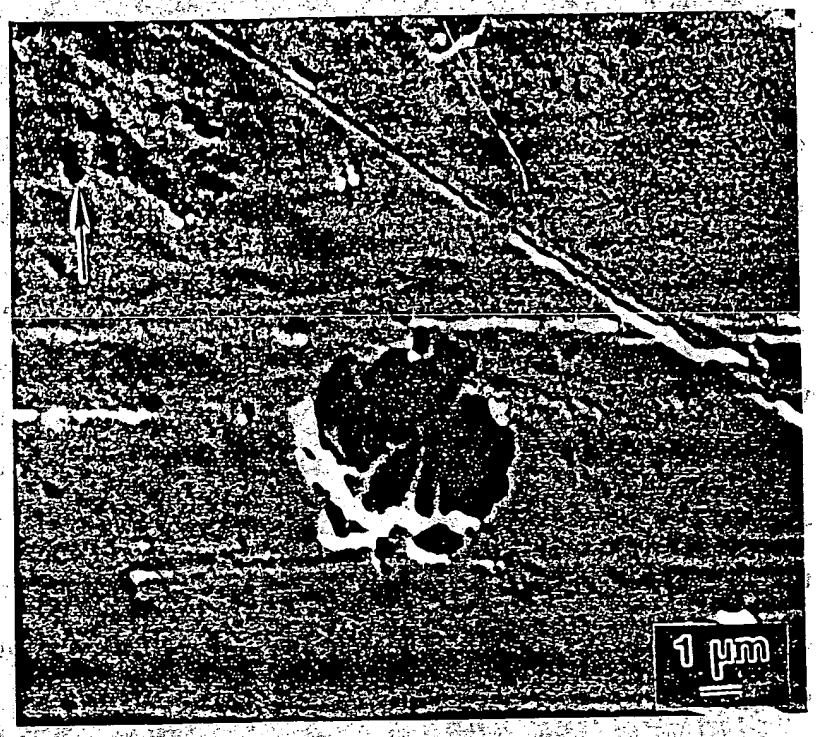

Fig. 2 SEM photo of a Pd cathode on the side facing the anode after electrolysis for 12 minutes. The large pit is thought to be the result of localized melting which occurred during electrolysis. The horizontal lines were caused by the cold rolling process which preceded electrolysis. Note that the large pit is not extended in the direction of the horizontal lines. This minimizes the possibility that the pit was present before electrolysis. Pits such as that indicated by the arrow were examined with the STM and AFM.

force mode, which means that vertical dimensions are captured in the nano-Newton scale, and the other being the height mode, which means that vertical dimensions are captured in the nanometer scale. The latter mode represents the surface height. Height mode images appear less sharp than their force mode counterparts; however, definition of height is lost in the force mode images. Figures 3a and 3b respectively demonstrate macroscopic images of the unexposed palladium and the electrolyzed palladium cathode surfaces, captured in the force mode. The unexposed surface at 10 μm dimensions exposes vertical lines, due to the cold-rolling action, while the electrolyzed cathode surface, seen at the same scale, exhibits a crater about 6 μm diameter. Figures 3c and 3d are increased magnifications of Fig. 3b, with scans at 6 μm and 2.5 μm, respectively. These images reveal crystal-like facets over the surface, where planes and nodules exist in various sizes. It seems that a high temperature process must have been involved in changing the surface morphology from that of Fig. 3a to that of Fig. 3b. The rounded, faceted features which are clearly visible in Figs. 3c and 3d most probably were caused by localized melting and subsequent crystallization at the cathode surface.

Figures 4a and 4b are height mode images of Fig. 3b. These images demonstrate clearly the height variation of the crater. The rim towers above the rest of the surface, while the interior portion recesses to form a cavity. This formation suggests that

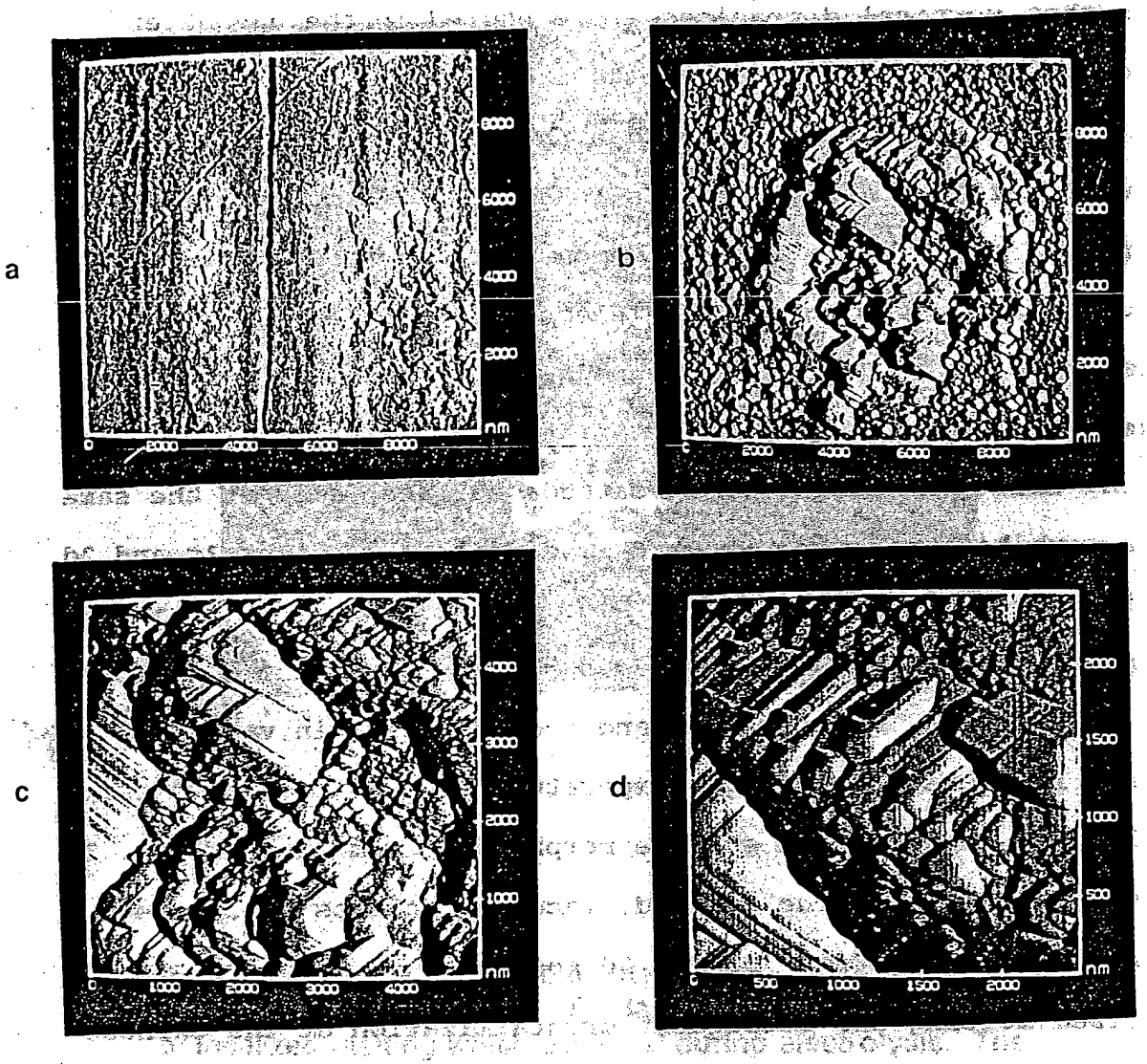

Fig. 3 AFM images of (a) Pd foil surface after cold rolling. The vertical lines resulted from contact with the steel rolls. (b) Pd cathode surface after electrolysis for 12 minutes. (c) and (d) Enlargements of the surface pit in (b) to show the rounded and faceted features.

a

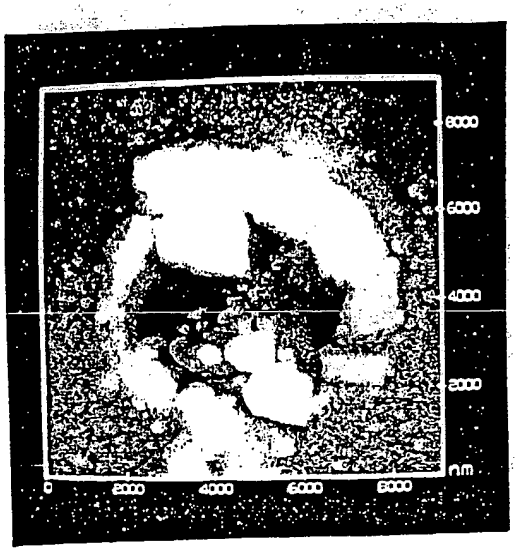

b

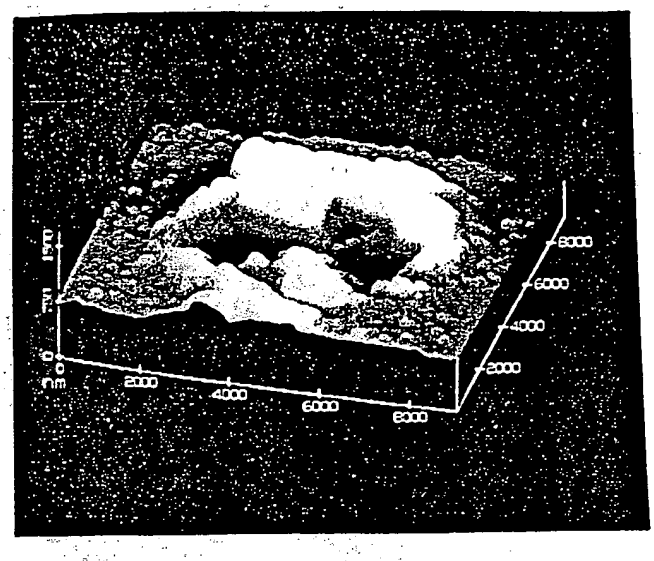

Fig. 4 Height mode images of Fig. 3b, showing that this feature is a crater with a rim.

the surface had undergone a dynamic change, one involving an energy transaction, such as localized melting.

Figures 5a through 5c show another crater on the electrode surface. Figure 5a illustrates in the height mode a bowl-shaped cavity on the surface, and Fig. 5b illustrates the same crater in the force mode, showing striations which converge into its center. Figure 5c is a line section of Fig. 5a, which places two arrows on the line that represents the contour of the crater. The flat region of the line demonstrates that the AFM cantilever tip could not reach the bottom of the approximately 1800 nm diameter well, making the drop significantly more than 260 nm from the rim.

Figures 6a and 6b, in the AFM force mode, respectively show other areas of the cold rolled Pd foil and the electrolyzed Pd cathode surfaces. Line boundaries of crystal facets can be seen once again on the electrode, as well as nodules. The facets intersect at about 71°, as in Figs. 3 and 5, suggesting that the straight boundaries are (111) plane traces. The vertical lines due to the cold-rolling action seen on the blank sample disappear again on the cathode surface, indicating that some morphological change has taken place. A line section of Fig. 6b in the height mode indicates that the lagoon-shaped configuration is really another pit, dropping more than 0.5 μm from the rest of the surface, and that it is accompanied by a rim that projects above it and the remaining surface (Fig. 6c).

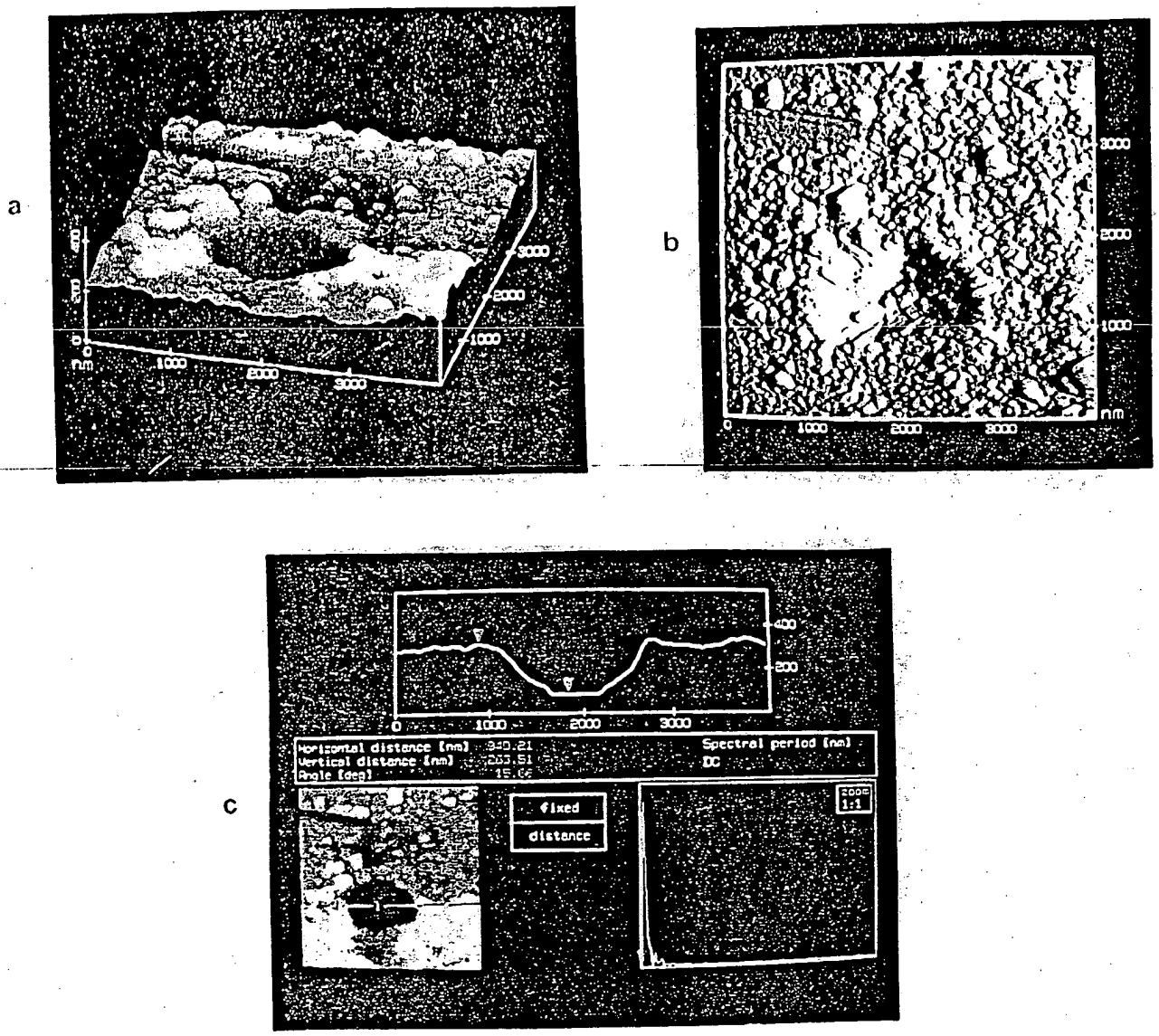

Fig. 5 (a) A bowl-shaped cavity in the Pd cathode, illustrated in the height mode. (b) The same crater in the force mode, showing striations which converge into its center. (c) Contour of the crater. The AFM tip did not reach the bottom of the crater.

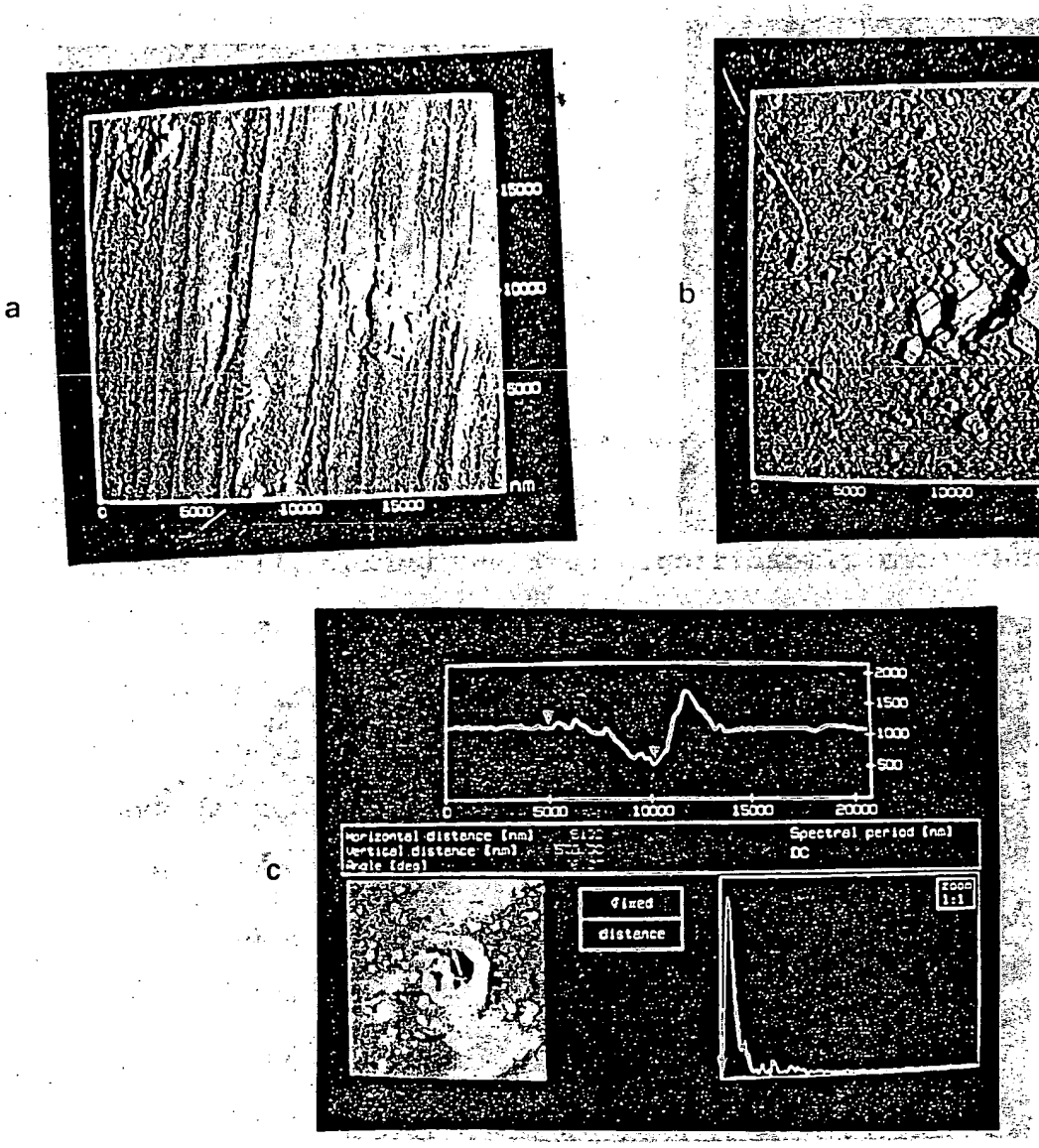

Fig. 6 Force mode micrographs of (a) cold rolled Pd and (b) electrolyzed Pd cathode. Using the height mode, a profile of the pit in (b) is shown in (c).

Figure 7 shows another AFM force mode image with smaller faceted particles whose boundaries again are consistent with (111) planes.

The scanning tunneling microscope, the predecessor of the AFM, relies principally upon a tunneling current, rather than electrostatic repulsion, between a platinum-iridium tip and the sample surface for imaging. Observations were again made in air at room temperatures using a Nanoscope II microscope.

Generally STM images of the cold rolled palladium foil and the electrolyzed palladium cathode yielded those seen in Figures 8a and 8b, respectively. The electrolyzed cathode clearly possesses the more detailed surface, seen at 4 μm by 4 μm dimensions. It displays in the height mode pores of over 10 nm diameter, whereas the cold rolled Pd is largely intact. Others who claim to see this effect using the STM believe that hydrogen ions are actually adsorbed and reduced on the surface. Some of these permeate into the Pd structure, producing porosity (4). These ions accumulate into the regions separated by lattice defects and cause them to swell. These swelled regions, along with craters, were typically observed with the STM.

Figure 9a presents another STM image of the electrolyzed Pd cathode at a 1 μm by 1 μm scale. A nodule is seen to contain more nodules, and pits form among them. Figure 9b shows a pit approximately 200 nm wide and more than 30 nm deep, which is typically seen in this region.

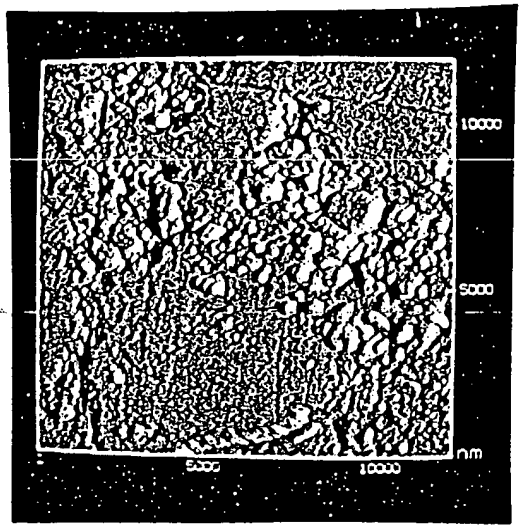

Fig. 7 Another AFM force mode image, unveiling irregular features on the electrode surface. Regions of nodules, furrows, and bluffs create greater surface area.

a

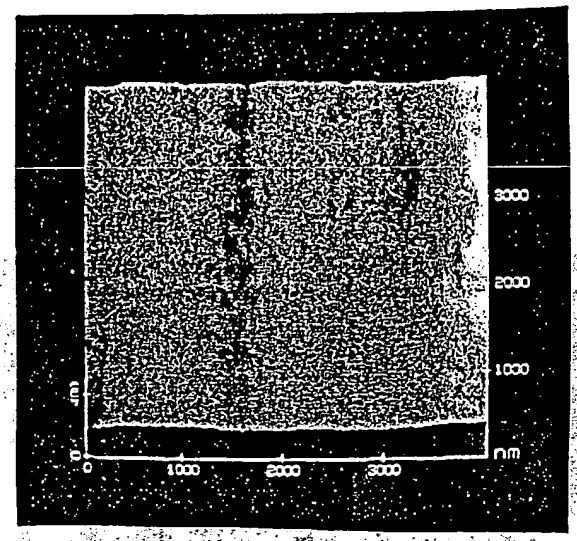

b

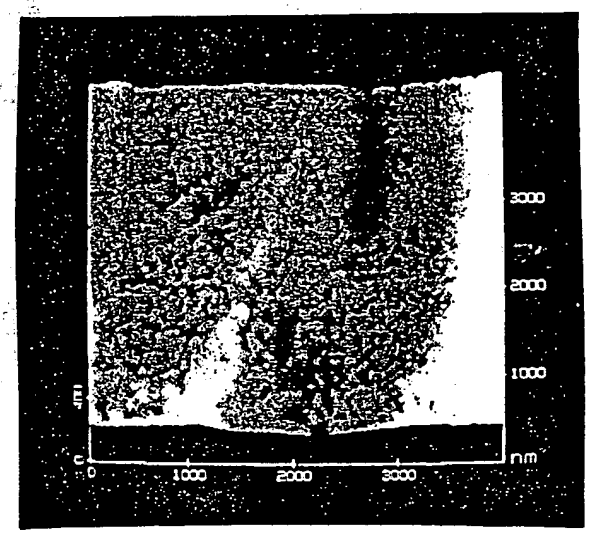

Fig. 8 STM images of (a) cold rolled Pd foil and (b) electrolyzed Pd cathode. Porosity is clearly visible in (b) but not in (a).

a

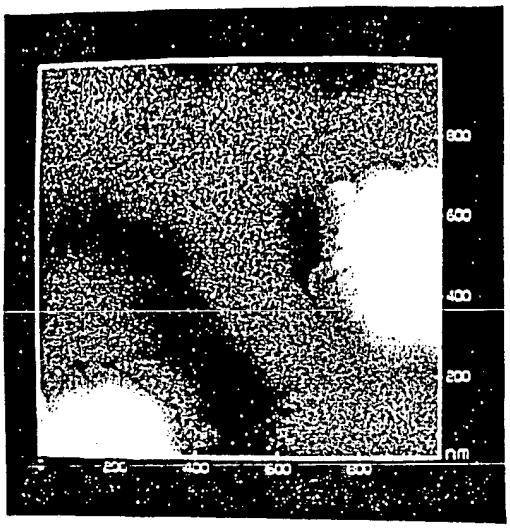

b

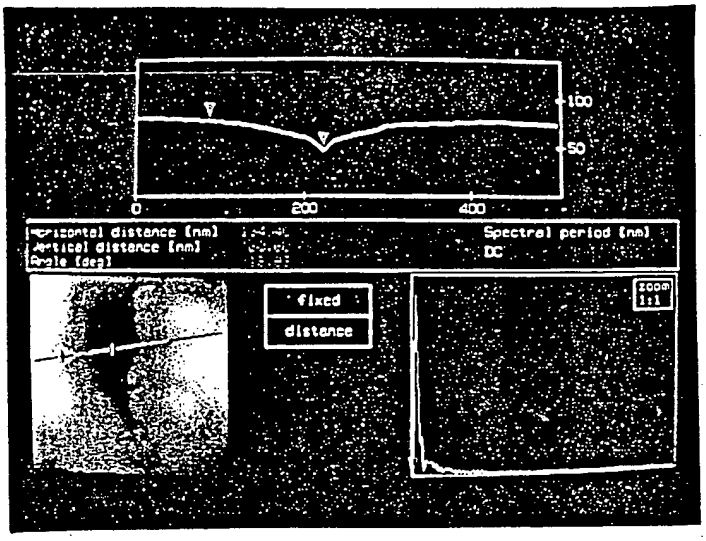

Fig. 9 (a) STM image of electrolyzed Pd cathode, showing microscopic pits. (b) Profile of one of the pits in (a).

DISCUSSION OF RESULTS

The results above document the microscopic changes in the surface morphology of a Pd cathode after electrolysis for 12 minutes in an electrolyte containing appreciable amounts of hydrogen ions along with deuterium ions. The surface craters observed with the SEM and AFM, especially, have characteristics such as stalagmites and rounded and faceted crystals which could be the result of localized melting. The height mode images and depth profiles showing rims around the craters suggest that molten material was ejected and solidified around the craters. Photos such as those in Figs. 4-6 illustrate microscopic events which are reminiscent of large-scale events such as the appearance of Mount St. Helens after the 1980 eruption. Other possibilities which could cause surface damage include chemical interaction with the electrolyte or mechanical damage caused by the formation of palladium hydride or deuteride. Chemical interaction is ruled out by the observation that palladium is chemically inert in the electrolyte (Fig. 1). Surface rupture might result from swelling caused by hydride or deuteride formation, but linear cracking, rather than cratering, would be the likely result. For example, a pattern of surface cracks forms when chromium hydride forms during electroplating of chromium (5). The surface of electroplated chromium has a nodular appearance, but there is no evidence of surface craters.

STM studies have been performed ex situ of the surface of a Pd cathode after electrolysis in aquaeous H_2SO_4 (1.5 mol dm^{-3}) for three hours with constant cathodic current density of 500 mA cm^{-2} (4). The surface changed from smooth to nodular, but these workers gave no evidence for cratering.

When a control cell with electrolyte containing light water and sulfuric acid is electrolyzed in series with the heavy water cell, the macroscopic distortion of the thin-foil Pd cathodes is of the same type in the two cells but much less in the light water cell than in the heavy water cell. Along with the greater distortion, the temperature of the heavy water cell increases more than that of the light water cell. These effects are quite reproducible (6, 7). Thus, a heavy water cell with a Pd cathode reproducibly undergoes more macroscopic distortion and generates more heat than an identical light water cell connected in series with the same amount of power entering both cells. The distortion is apparently caused by compressive stresses on the cathode surface which faces the anode during electrolysis. Compressive stresses could be produced by porosity resulting from swelling of the lattice when hydrogen or deuterium is absorbed. Reaction of these gases with Pd results in formation of the beta phase, which has a lattice parameter about 3.6% larger than Pd. The cause of greater macroscopic distortion during heavy water electrolysis could be the observed cratering which may result from localized melting.

This Page is Inserted by IFW Indexing and Scanning Operations and is not part of the Official Record

BEST AVAILABLE IMAGES

Defective images within this document are accurate representations of the original documents submitted by the applicant.

Defects in the images include but are not limited to the items checked:

- ☐ **BLACK BORDERS**
- ☐ **IMAGE CUT OFF AT TOP, BOTTOM OR SIDES**
- ☐ **FADED TEXT OR DRAWING**
- ☐ **BLURRED OR ILLEGIBLE TEXT OR DRAWING**
- ☐ **SKEWED/SLANTED IMAGES**
- ☐ **COLOR OR BLACK AND WHITE PHOTOGRAPHS**
- ☐ **GRAY SCALE DOCUMENTS**
- ☐ **LINES OR MARKS ON ORIGINAL DOCUMENT**
- ☐ **REFERENCE(S) OR EXHIBIT(S) SUBMITTED ARE POOR QUALITY**
- ☐ **OTHER:** _____

IMAGES ARE BEST AVAILABLE COPY.

As rescanning these documents will not correct the image problems checked, please do not report these problems to the IFW Image Problem Mailbox.